Development and demonstration of wind turbine fault ride through capability

The penetration of wind generation has increased in many areas to a significant level. In such areas, modern wind turbines are required to be able to endure deep voltage dips. Otherwise, major problems to the power systems stability would occur. In addition to staying connected during the fault, modern wind turbines should be able to support the grid voltage during the voltage dip by injecting reactive power.

Two most common variable speed wind turbine types are the doubly-fed induction generator (DFIG) wind turbine and wind turbine with full-power converter interface to the grid, Fig. 1. However, the behavior of the concepts during the grid voltage dip differ significantly. The DFIG suffers from high rotor voltages and currents. Hence, the converter connected to the rotor windings may have to be disconnected in order to protect the converter. Then, the wind turbine is not controllable anymore which complicates the reactive power injection for network voltage support.

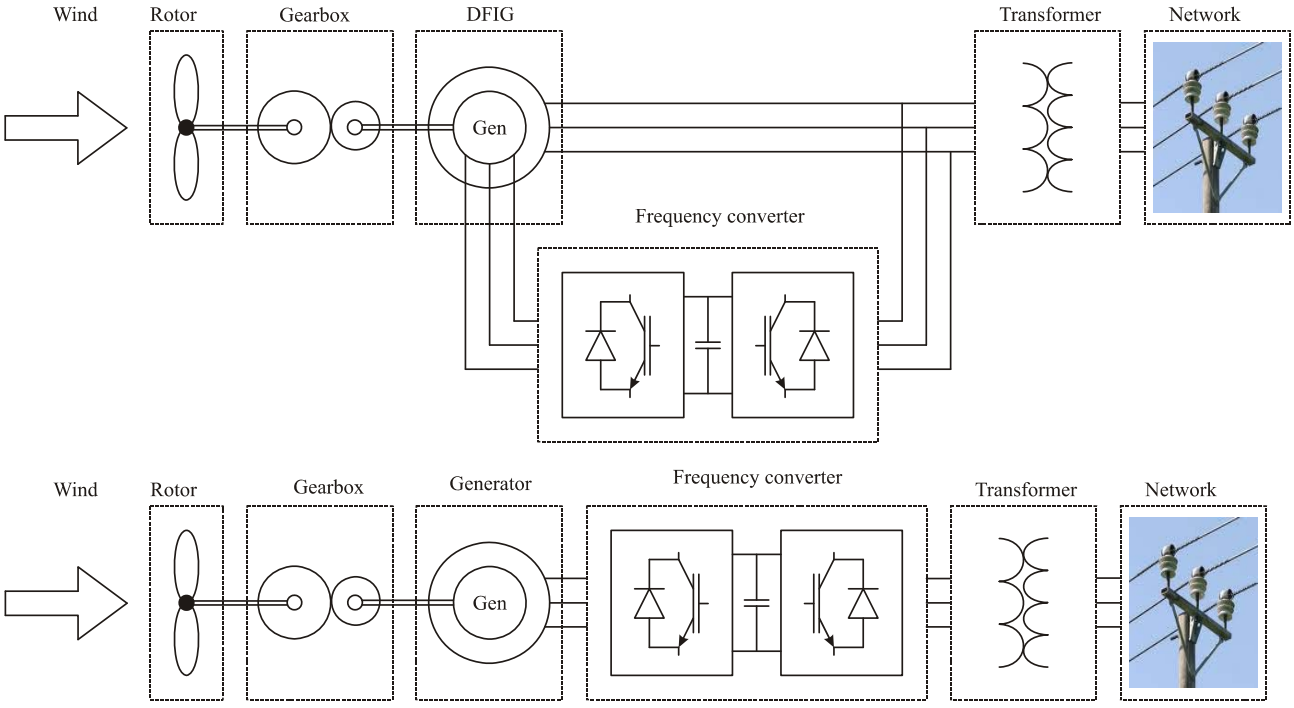

Fig. 1. Doubly-fed induction generator wind turbine concept and full-power converter wind turbine concept.

1. DFIG model

Doubly fed induction generators (DFIG) are used for variable speed wind turbines since the size and costs of the power electronic devices are smaller compared to full power converter design wind turbine. In addition, the losses are reduced. In the concept, the stator of the generator is connected directly to the grid while the rotor circuit is connected to the grid via frequency converter. This topology allows the generator to operate with slips between -0.3 and 0.3. When the slip has positive value the direction of the slip power, i.e. power in the rotor circuit, is from the grid towards the rotor and when the slip is negative the slip power direction is towards the grid. Thus, it is more beneficial to operate with negative slip. The maximum slip power is 30 % of the wind turbine nominal power. Since the frequency converter is sized according to slip power, the converter rating is 30 % of the wind turbine nominal power. Main drawbacks of the concept are the need of slip rings and operation during grid faults. [1]

The space vector based DFIG topology is represented in Fig. 2. The nominal power of the modelled DFIG wind turbine is 1.7 MVA. Typical parameters for wind turbine rotor, gearbox, generator, frequency converter and LCL-filter are received from real manufacturer. Table 1 depicts the used parameters. The modelling of is done using MatLab/Simulink.

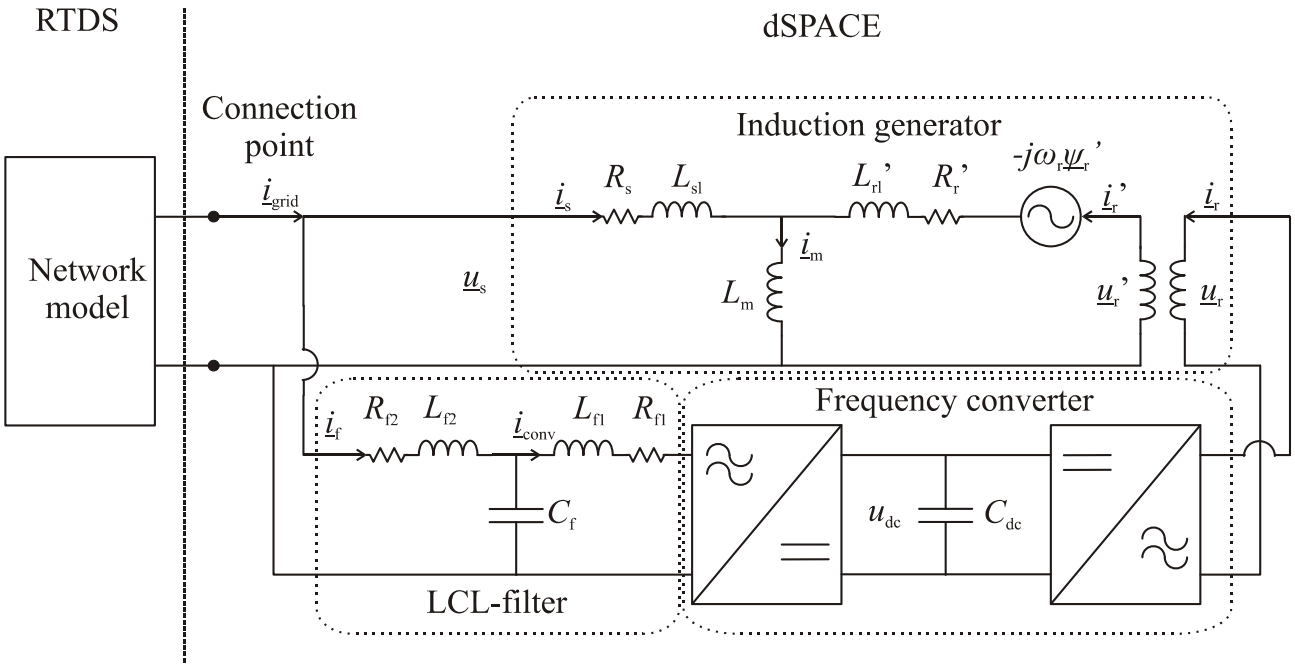

Fig. 2. Equivalent circuit of the DFIG wind turbine concept.

Table 1. Simulation parameters.

Stator resistance: $R_s = 0.0027\ \Omega$	Rotor resistance: $R_r = 0.0026\ \Omega$
Stator leakage reactance: $X_{sl} = 0.028\ \Omega$	Rotor leakage reactance: $X_{lr} = 0.029\ \Omega$
Magnetizing reactance: $X_m = 1.2\ \Omega$	Rotor to stator turns ratio: $N_r/N_s = 2.73$
Polepairs: $p = 2$	Wind turbine radius: $r = 38$ m
Total inertia constant reduced to generator shaft: $J = 500\text{kgm}^2$	Gearbox transmission ratio: $n = 100$
Friction constant: B = 3.18 Nms/rad	
Dc-link capacitor: $C_{dc} = 22$ mF	Dc-link voltage: $u_{dc} = 1000$ V
Converter side filter inductance: $L_{f1} = 190\ \mu$H	Grid side filter inductance: $L_{f2} = 125\ \mu$H
Filter capacitor: $C_f = 70\ \mu$F	

Rotor

The wind turbine rotor is modelled based on equation (1). Wind speed variations may locally have very high frequency. In addition, the variations are local with respect to large rotor swept area. Thus, high frequency variations even out. This smoothing effect is modelled by using a first order low pass filter after wind model as in [1]. In this case, the time constant of 1 second was used. Figure 3 shows the low pass filter model.

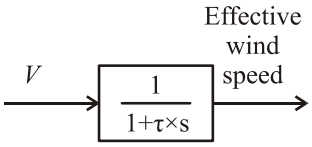

Fig. 3. Filter model to describe wind speed smoothing in rotor.

The performance coefficient $c_p(\lambda,\theta)$ is calculated from the following equation: [1]

$$c_p(\lambda,\theta) = 0.73\left(\frac{151}{\lambda_i} - 0.58\times\theta - 0.002\times\theta^{2.14} - 13.2\right)e^{\left(\frac{-18.4}{\lambda_i}\right)} \quad (1)$$

where

$$\lambda_i = \left[\left(\frac{1}{\lambda - 0.02\times\theta}\right) - \left(\frac{-0.003}{\theta^3+1}\right)\right]^{-1} \quad (2)$$

A lumped mass drive train model is used to illustrate the mechanical parts of the wind turbine system.

Doubly Fed Induction Generator

Doubly fed induction generator is modelled in a stationary reference frame based on the equivalent circuit shown in the Fig. 2. Stator voltages and rotor voltages reduced to the stator can be expressed as follows: [2]

$$\begin{aligned} \underline{u}_\mathrm{s} &= R_\mathrm{s}\underline{i}_\mathrm{s} + \frac{d\underline{\psi}_\mathrm{s}}{dt} \\ \underline{u}_\mathrm{r}' &= R_\mathrm{r}'\underline{i}_\mathrm{r}' + \frac{d\underline{\psi}_\mathrm{r}'}{dt} - \mathrm{j}\omega_\mathrm{r}\underline{\psi}_\mathrm{r}' \end{aligned} \quad (3)$$

where R_s and R_r are stator resistance and rotor resistance respectively, $\underline{\psi}_\mathrm{s}$ and $\underline{\psi}_\mathrm{r}$ are stator and rotor flux linkage respectively, $\underline{i}_\mathrm{s}$ and $\underline{i}_\mathrm{r}$ are stator current and rotor current respectively and ω_r is the angular speed of the rotor. Superscript ‘ means that the variable is reduced to stator. Reduction is done as follows:

$$\begin{aligned} \underline{u}_\mathrm{r} &= N\underline{u}_\mathrm{r}' \\ \underline{i}_\mathrm{r} &= \frac{1}{N}\underline{i}_\mathrm{r}' \\ R_\mathrm{r} &= N^2 R_\mathrm{r}' \\ L_\mathrm{rl} &= N^2 L_\mathrm{rl}' \end{aligned} \quad (4)$$

Flux linkages can be expressed: [2]

$$\begin{aligned} \underline{\psi}_\mathrm{s} &= (L_\mathrm{m} + L_\mathrm{sl})\underline{i}_\mathrm{s} + L_\mathrm{m}\underline{i}_\mathrm{r}' = L_\mathrm{s}\underline{i}_s + L_\mathrm{m}\underline{i}_\mathrm{r}' \\ \underline{\psi}_\mathrm{r}' &= (L_\mathrm{m} + L_\mathrm{rl}')\underline{i}_\mathrm{r}' + L_\mathrm{m}\underline{i}_\mathrm{s} = L_\mathrm{r}'\underline{i}_\mathrm{r}' + L_\mathrm{m}\underline{i}_\mathrm{s} \end{aligned} \quad (5)$$

2. Control systems of the wind turbine

The control system of wind turbine is divided into three parts. The pitch control system is used to curtail wind power production during high wind speeds in order to reduce the load of mechanical and electrical parts of the wind turbine system. Rotor side converter adjusts the speed of wind turbine such that energy production is maximized. That is reached by optimizing the tip speed ratio λ which is the ratio between wind turbine tip speed and the wind speed. Grid side converter maintains constant dc-link voltage and controls the reactive power exchange with the grid.

Rotor Side Converter Control

The control system of the rotor side converter is shown in Fig. 4. [3] The converter is controlled in a reference frame that is oriented to the stator flux. Thus, it is possible to control the generators active and reactive power independently. The stator flux vector angle θ_ms is obtained from the stator voltage equations: [2]

$$\psi_{s\alpha} = \int (u_{s\alpha} - R_s i_{s\alpha})dt$$
$$\psi_{s\beta} = \int (u_{s\beta} - R_s i_{s\beta})dt \quad (6)$$

$$\theta_{ms} = \tan^{-1}\frac{\psi_{s\beta}}{\psi_{s\alpha}} \quad (7)$$

The reference value for the speed controller is obtained by optimizing the tip speed ratio. The output is the reference value for the electrical torque $t_{e,ref}$.

Instantaneous electrical torque in stator flux coordinates is expressed: [2]

$$t_e = \frac{3}{2} p \psi_{sx} i_{sy} = \frac{3}{2} p L_m |\underline{i}_{ms}| i_{sy} . \quad (8)$$

It can be seen that the electrical torque is directly proportional to the y-component of the stator current. Y-component of the rotor current is proportional to the y-component of the stator current:

$$i_{sy} = -\frac{L_m}{L_s} i_{ry} . \quad (9)$$

Thus, the output of the torque controller is the reference value for the rotor current y-component.

Rotor voltage equations in the stator flux coordinates are:

$$\begin{aligned} \underline{u}_r' &= R_r' \underline{i}_r' + L_r' \frac{d\underline{i}_r'}{dt} + L_m \frac{d\underline{i}_s}{dt} + j(\omega_{ms} - \omega_r)(L_r' \underline{i}_r' + L_m \underline{i}_s) \\ &= R_r' \underline{i}_r' + \sigma L_r' \frac{d\underline{i}_r'}{dt} + j\omega_{sl}\left(\sigma L_r' \underline{i}_r' + \frac{L_m^2}{L_s}|\underline{i}_{ms}|\right) \end{aligned} \quad (10)$$

where $\sigma L_r'$ is a transient inductance ($\sigma L_r' = L_r' - L_m^2/L_s$), ω_{sl} is a slip frequency ($\omega_{sl} = \omega_{ms} - \omega_r$), $\underline{i}_{ms}$ is a stator magnetizing current ($\underline{i}_{ms} = (L_s/L_m) * \underline{i}_s + \underline{i}_r'$) and the magnetizing current is assumed to be a constant ($d|\underline{i}_{ms}|/dt = 0$). The equation (10) can be expressed in component form: [2]

$$\begin{aligned} u_{rx}' &= R_r' i_{rx}' + \sigma L_r' \frac{di_{rx}'}{dt} - \omega_{sl} \sigma L_r' i_{ry} \\ u_{ry}' &= R_r' i_{ry}' + \sigma L_r' i_{rx}' \frac{di_{ry}'}{dt} + \omega_{sl}\left(\sigma L_r' i_{rx}' + \frac{L_m^2}{L_s}|\underline{i}_{ms}|\right) \end{aligned} . \quad (11)$$

From the equation (11) it can be seen that rotor voltage component can be controlled by controlling the respective current if cross-coupling terms are removed. This is done by adding cross-coupling term to the output of the controller.

$$u_{\mathrm{rx}}{}'_{,\mathrm{ref}} = u_{\mathrm{rx}}{}' - \omega_{\mathrm{sl}}\sigma L_{\mathrm{r}}{}' i_{\mathrm{ry}} = R_{\mathrm{r}}{}' i_{\mathrm{rx}}{}' + \sigma L_{\mathrm{r}}{}' \frac{di_{\mathrm{rx}}{}'}{dt}$$
$$u_{\mathrm{ry}}{}'_{,\mathrm{ref}} = u_{\mathrm{ry}}{}' + \omega_{\mathrm{sl}}\left(\sigma L_{\mathrm{r}}{}' i_{\mathrm{rx}}{}' + \frac{L_{\mathrm{m}}{}^2}{L_{\mathrm{s}}}\left|\underline{i}_{\mathrm{ms}}\right|\right) = R_{\mathrm{r}}{}' i_{\mathrm{ry}}{}' + \sigma L_{\mathrm{r}}{}' i_{\mathrm{rx}}{}' \frac{di_{\mathrm{ry}}{}'}{dt} \quad (12)$$

Thus, reference voltages of the rotor side converter are:

$$u_{\mathrm{rx,ref}} = N u_{\mathrm{rx}}{}'_{,\mathrm{ref}}$$
$$u_{\mathrm{ry,ref}} = N u_{\mathrm{ry}}{}'_{,\mathrm{ref}} \quad (13)$$

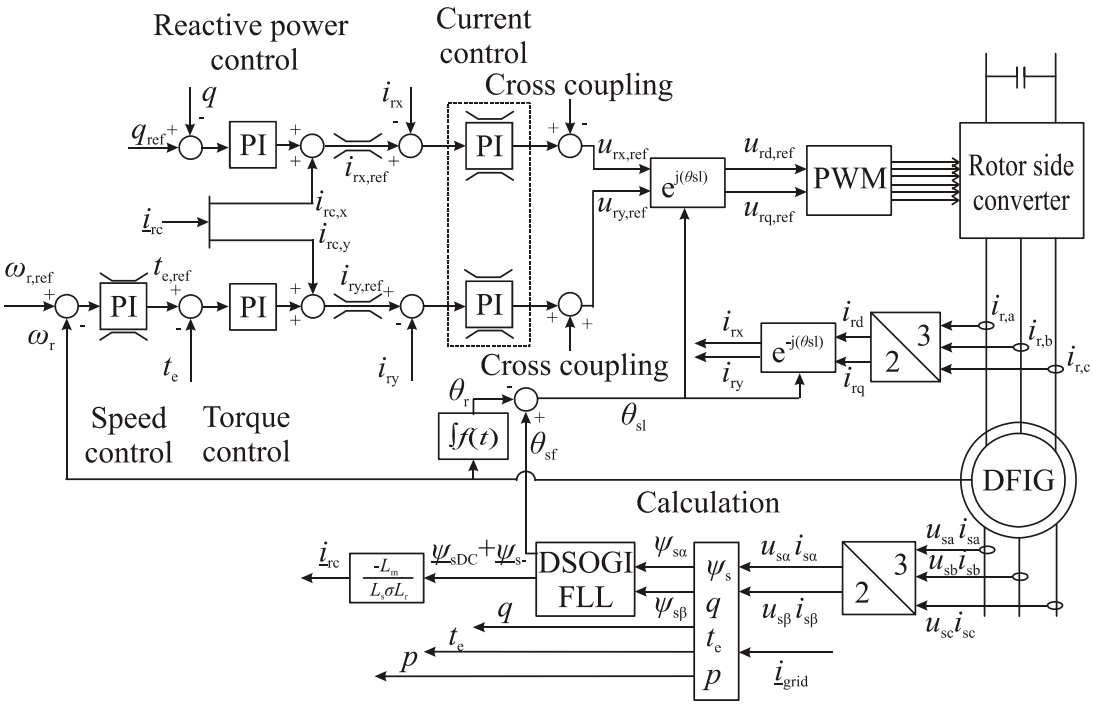

Fig. 4. The control system of the rotor side converter.

Grid Side Converter control

The aim of the grid side converter control is to keep the dc link voltage constant, thereby ensuring that the active power generated by the generator is fed to the network. Additionally, it is possible to control the reactive power fed to the grid.

The grid side converter is controlled in a synchronous reference frame that rotates synchronously with the connection point voltage vector $\underline{u}_{\mathrm{m}}{}'$. The phase angle of the fundamental frequency component of the connection point voltage is extracted using phase-locked loop (PLL) [4]. The control strategy is implemented, similarly as in the case of generator side converter, with two cascade loops. The fast inner loop controls the grid current $\underline{i}_{\mathrm{conv}}$ and the outer loop controls the dc link voltage u_{dc}. The control system is presented in Fig. 5.

The dc link voltage reference $u_{\mathrm{dc}}{}^*$ is compared to the actual measured voltage u_{dc}. The dc-link voltage error is fed to the PI-controller as an input and a direct axis current reference $i_{\mathrm{conv,x}}{}^*$ is obtained. The current

reference of the x-axis component is then compared to the measured current $i_{conv,x}$ and the error current is fed to the current PI-controller.

The reactive power transferred to the network can be regulated with the quadrature axis current component $i_{conv,y}$. The target of the reactive power control is, in this case, to produce unity power factor to the connection point of the wind turbine system. The unity power factor in connection point is achieved when $i_{f2,y}$ is zero, see Fig. 2. Thus, the current flow through a filter capacitor must be taken into account. In the study, the value for the reference current $i_{conv,y}^*$ is determined empirically with the help of iterative simulations.

The reference current $i_{conv,q}$* is compared to measured current $i_{conv,y}$ and the current error is fed to the current PI-controller. The output of the current controller is the reference voltage over the two filter inductors $\underline{u}_{Lf}^*$. Removing the cross-coupling terms and with the help of the measured connection point voltage $\underline{u}_m'$, the converter voltage reference $\underline{u}_{conv}^*$ can be presented.

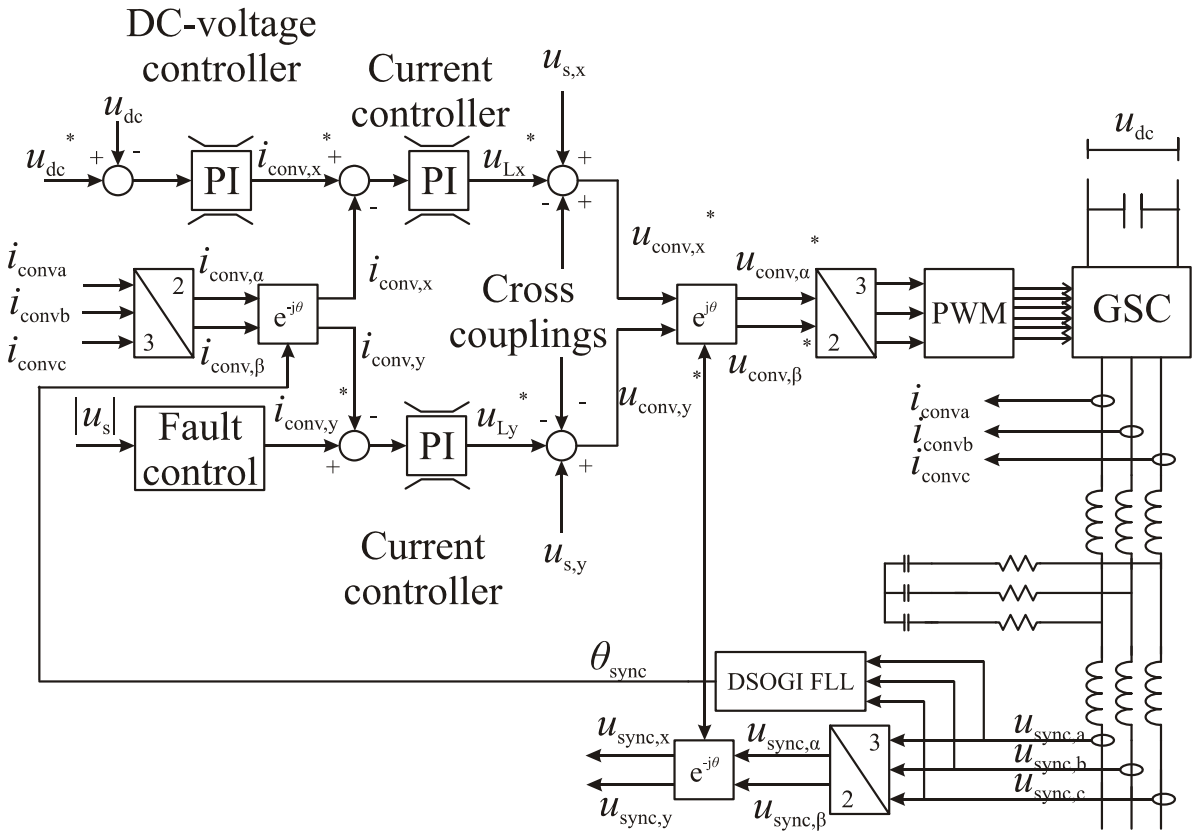

Fig. 5. Grid side converter control.

Pitch control

When instantaneous active power p fed to the network is lower than nominal active power p_N of the turbine the pitch angle is kept zero. After the active power output exceeds the nominal value the power production is reduced. The power production of the wind turbine is decreased by increasing the blade pitch angle. The low pass filter with time constant of 1.2 seconds represents the actuator of the pitching system. The rate of

pitching is limited to 10° per second which is prevalent pitching speed according to [5]. Figure 6 illustrates the pitch control system. [6]

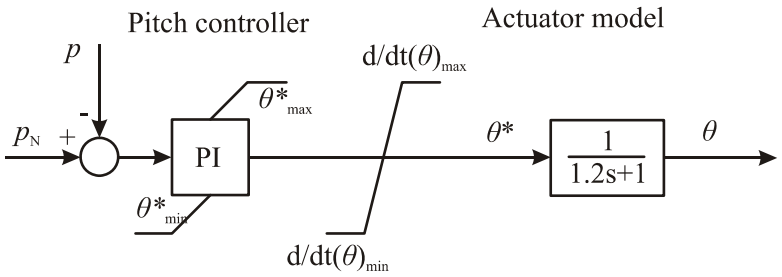

Fig. 6. Pitch control system.

3. Full power converter permanent magnet synchronous generator wind turbine

Wind turbine concept that uses permanent magnet synchronous generator and full power converter has become more favourable in recent days. The generator has high efficiency since no power is needed to magnetize the generator. The controllability of the wind turbine concept is excellent, which is significant benefit, since according to grid codes modern wind turbines must have capability to provide controllable active and reactive power. [7] However, the weakness of the concept is high costs. Permanent magnets are very expensive and the costs of large frequency converter that is sized to handle nominal power of the wind turbine are substantial.

Modelling of wind turbine

Figure 7 illustrates the modeled space-vector based wind power system. The rotor extracts kinetic energy from the wind and converts it into rotational energy of the rotor shaft. The gearbox between the rotor and the generator is used to increase the rotational speed of the shaft suitable for the generator. The permanent magnet synchronous generator (PMSG) is connected to the grid through a back-to-back voltage source converter. The generator side converter controls the generator stator current and the rotor shaft speed. The function of the grid side converter is to control the active and reactive power, which is transferred to the grid via an LCL-filter. An ideal step-up transformer is used to match the voltage level to the medium voltage network, which consists of RL-load, two Raven wires and grid. The grid is modeled as a three phase voltage source converted to space vectors. Modeling and control system details can be found from [8] and [9].

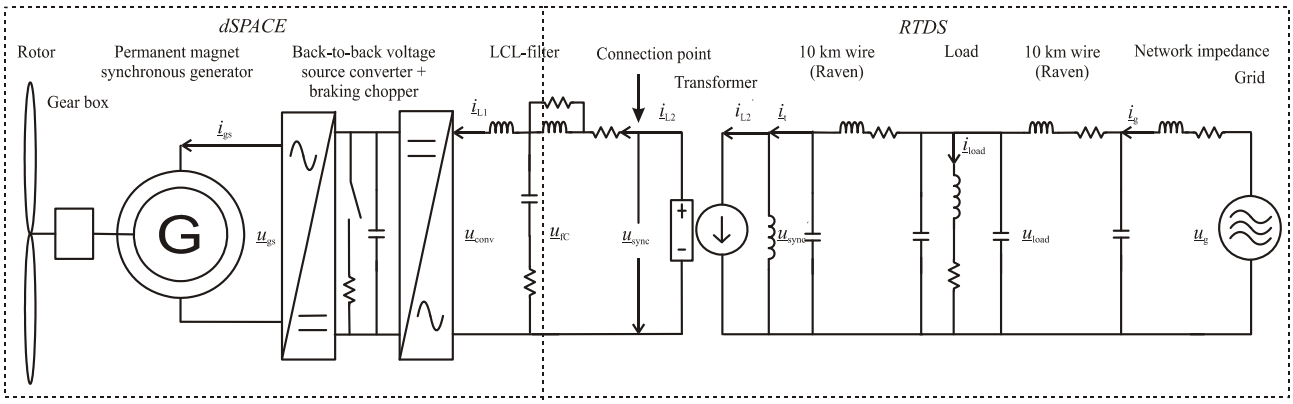

Fig. 7. The modeled wind power system.

4. Real time simulation environment

The real-time simulation environment consists of dSPACE DS1103 controller board, RTDS, a REF543 relay by ABB and amplifier Omicron CMS 156. The novel environment makes it possible to develop control strategies for WTs to qualify more demanding grid codes in the future. Minimization of the simulation time and the option to share calculation power between two simulators can be considered additional benefits. The aforementioned environmental properties enable simulations of more complex models. In addition, it is possible to use real protection relays as a part of a simulation system.

The dSPACE is designed for testing and developing fast mechatronics control systems. The dSPACE consists of a PowerPC processor, an additional DSP controller and plenty of interfaces including A/D and D/A channels, serial and CAN channels. In this study, Simulink is used to model the WT and the back-to-back VSC. The model is compiled to C-code and uploaded to dSPACE. The I/O hardware of dSPACE can be accessed through the Real-Time Interface library from Simulink. The real-time simulation is controlled and observed with the ControlDesk program.

RTDS is a digital electromagnetic transient power system simulator. The RSCAD software provides the user interface for RTDS hardware. The software consists of Draft and Runtime mode. Draft mode is used to model the network and associated controls. Based on the model, the RTDS makes the real-time simulation which can be controlled and observed in Runtime mode.

The relay utilized is ABB REF543 which, in these simulation studies, was configured to operate as a LOM relay. Over- and undervoltage (low stage (U<&U>) and high stage (U<<&U>>) settings), over- and underfrequency and rate of change in frequency (ROCOF) protection functions were included in the relay configuration. The hardware arrangement of the environment is shown in Fig. 8. [9]

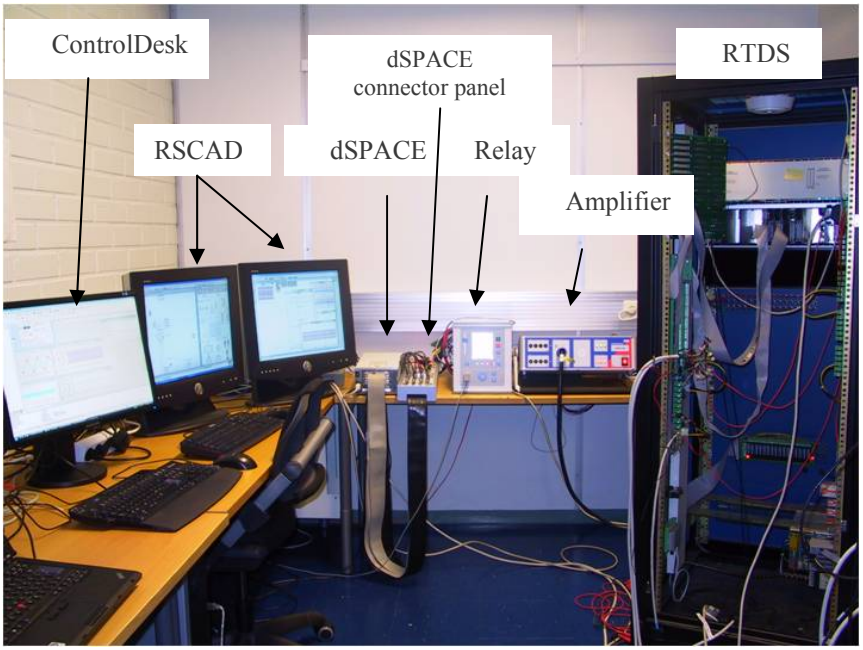

Fig. 8. The hardware arrangement of the Real-Time Simulation Environment.

DFIG in RTDS/dSPACE environment

Figure 9 shows the block diagram of the RTDS/dSPACE implementation. The DFIG is modelled in Simulink and based on the model dSPACE makes the simulation in real time. Program ControlDesk is used to control and observe the simulation. Power system model is created in RSCAD Draft mode. RSCAD Runtime mode is used to control the real time simulation that is performed by RTDS.

Data transmission between real time simulators is done through analog signals. In other words, first digital signals of the simulator is converted to analog signals which are converted back to digital signals when fed to other simulator. dSPACE receives connection point voltages $u_{s(a,b,c)}$ and interruption signal from RTDS and gives the connection point current $i_{grid(\alpha,\beta)}$ back. From the RTDS viewpoint, the wind turbine is modelled as a current source. The interruption signal *int* is used to synchronize the calculations of dSPACE and RTDS.

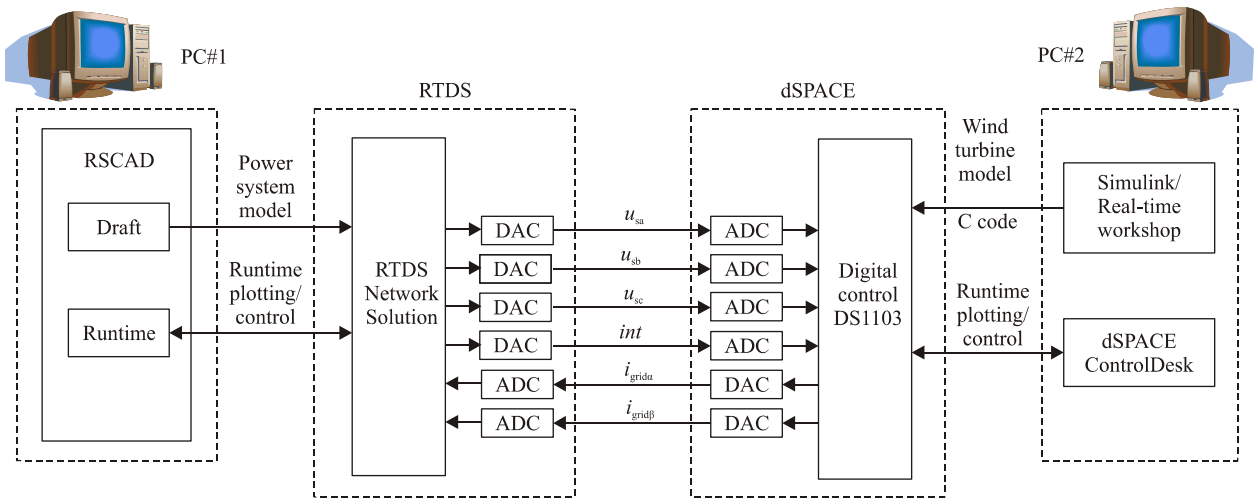

Fig. 9. Block diagram of the RTDS/dSPACE implementation.

Full power converter wind turbine in RTDS/dSPACE environment

Figure 10 depicts the practical implementation of the simulation environment. dSPACE receives connection point voltages $u_{sync(a,b,c)}$, connection point currents $i_{L2(a,b,c)}$ and information on whether the relay is open or closed (*Relay on*) from the RTDS. dSPACE sends back the voltage over the LCL-filter capacitor $u_{fC(a,b,c)}$ to RTDS. In other words, the WT system modeled in dSPACE is a voltage source in the RTDS. Data transmission between the simulators is done via analog signals. The connection point voltage measurement is fed from RTDS to the relay via amplifier. The amplifier is needed for amplifying the voltage signals coming from the digital to analog converter card (DDAC) of the RTDS unit since the output voltage range of the DDAC card (±10V) is not sufficient for the actual relay.

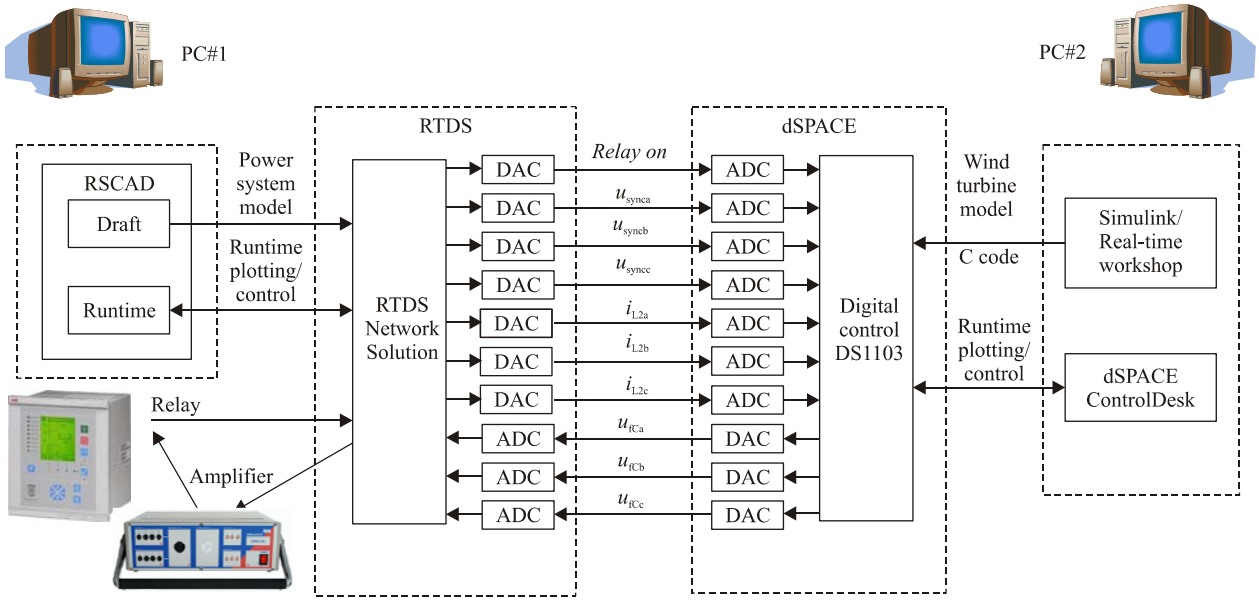

Fig. 10. Block diagram of the RTDS/dSPACE implementation.

5. Laboratory test setup

The circuit diagram of the laboratory test setup for wind turbine that uses permanent magnet synchronous generator and full power converter is shown in Fig. 11. The dc-motor is used to emulate the behavior of the wind turbine rotor. The dc-motor produces mechanical torque to the rotor shaft of the permanent magnet synchronous generator (PMSG). The torque of the dc-motor is control using dSPACE real-time simulator. The three level three wire generator side converter controls the speed of the PMSG. The dSPACE is responsible of the outer control loop, i.e., the speed control loop, and the output of the loop is the reference for stator current d- and q -components in a rotor reference frame. The current control system is implemented using Freescale MPC563 microcontroller. The microcontroller is located on the controller card in addition with the logic circuits for modulation signals, couplings for current and voltage measurements and current limiters. The connection between the controller card and the PC is done using series bus.

The three level four wire grid side converter controls the dc-link voltage to a constant value thereby assuring that no active power is stored in the dc-link. The control system is oriented to the synchronous reference frame which rotates with the network voltage. The control systems are implemented using MPC563 microcontroller. The GSC is connected to the network through LCL-filter. Third converter connected to the dc-link is the load side converter which feeds passive load. The three level four wire load side converter can be utilized in studies related to wind turbine operation during network islanding. The dSPACE can be used to activate and de-activate all converters. The used dc-motor, PMSG and generator side converter is shown in Fig. 12. In addition to islanding operation of wind turbine the laboratory test setup can be used in studies related to wind turbine operation during network faults and wind turbine voltage control.

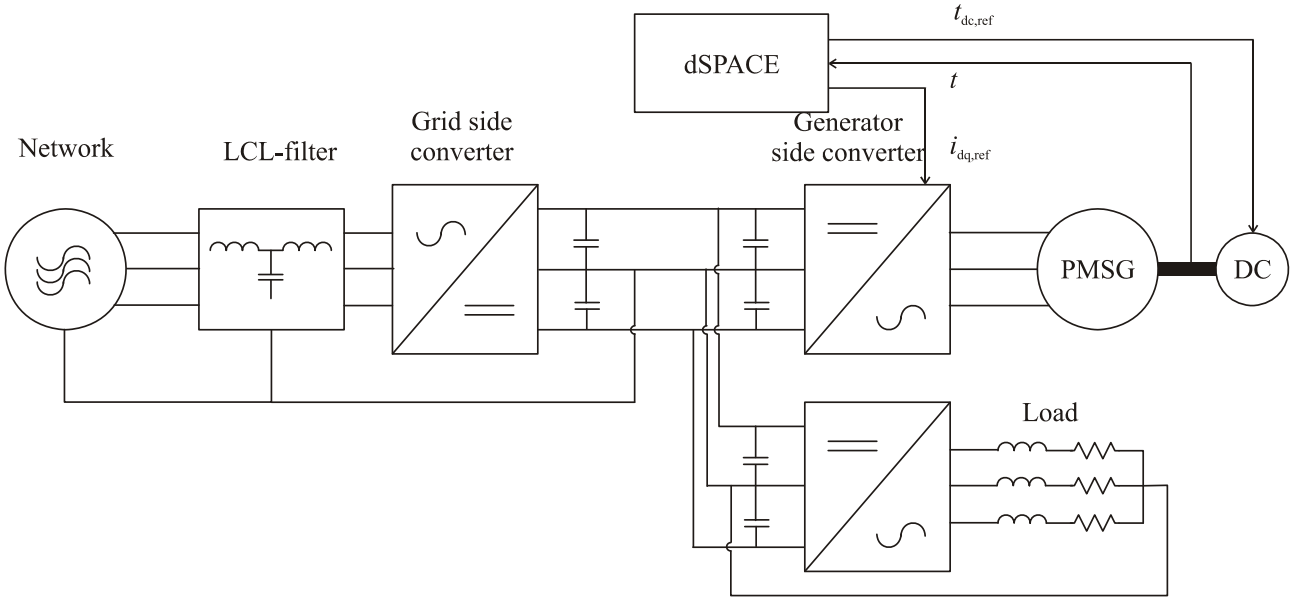

Fig. 11. The circuit diagram of the PMSG prototype.

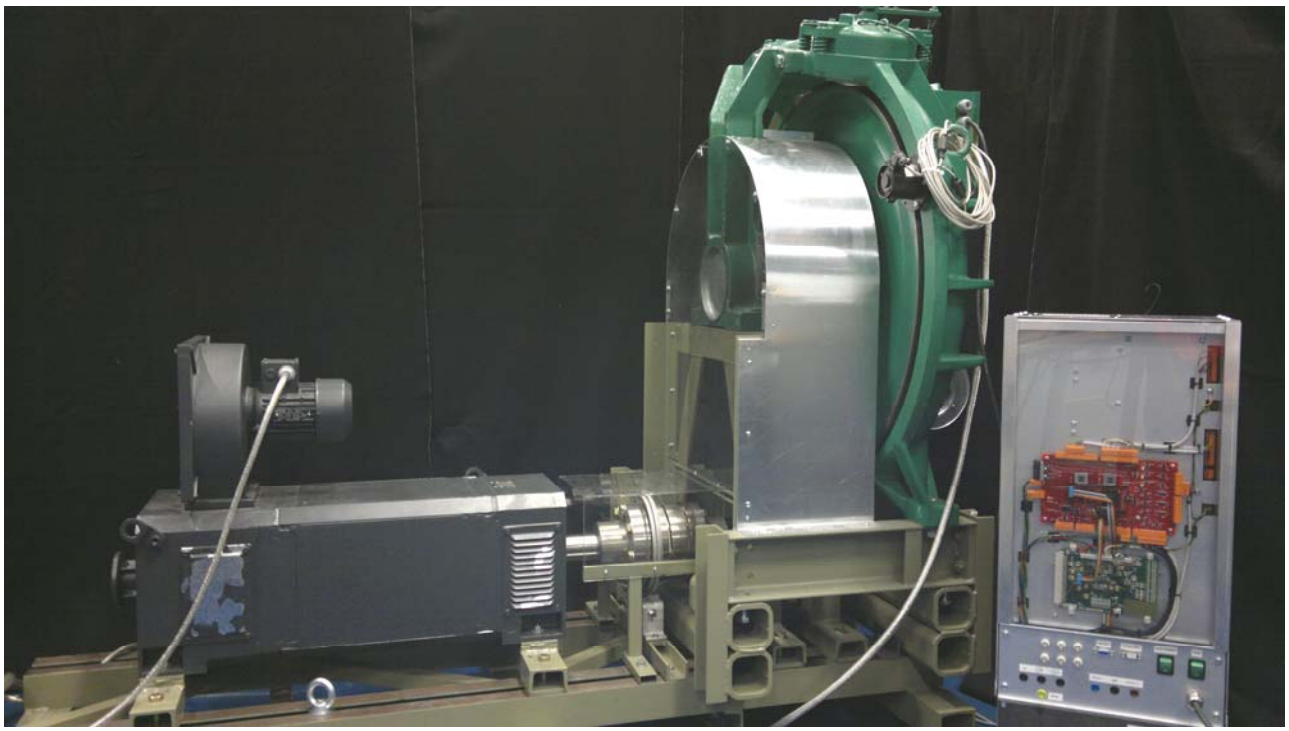

Fig. 12. The dc-motor, the permanent magnet synchronous generator and the generator side converter used in the laboratory test environment.

6. Fault ride through

The fault ride through capability of wind turbine topologies presented above has been studied using RTDS/dSPACE -environment. References [6], [8] and [9] discuss the operation of PMSG and full power converter wind turbine concept during a symmetrical grid fault. It is found that the concept is robust against network voltage sags and the fault ride through capability is achieved with quite simple control and protection actions. The fault ride through strategy used in studies [6], [9] relies on the intelligent control of the frequency converter and pitch angle. In addition, the braking chopper is installed to enhance the FRT. The wind turbine concept can also inject reactive power to the network during a voltage dip in order to support the depressed network voltage.

The FRT and reactive power support capability of DFIG wind turbine is studied in the reference [10]. The aim of the paper is to reveal how the compensation of transient flux enhances the performance of a DFIG wind turbine during a voltage dip. A comparison of two FRT strategies was made. The first FRT strategy uses only the active crowbar to protect the turbine and the second strategy uses transient flux compensation in addition to the crowbar. Simulations are carried out using Matlab/Simulink. Simulation results show that if the transient flux is compensated the DFIG show much steadier behaviour and the DFIG is controllable during a fault. Thus, it is possible to utilize the whole current capacity of the RSC for reactive power injection into the grid. This is an important aspect since the latest grid codes require reactive power injection into the grid during a voltage dip.

In reference [11] the influence of the DFIG fault ride through capability and reactive current injection to the operation of the wind turbine circuit breaker is studied. Due to the presence of non-rotating transient flux on the airgap of the generator the dc-component occurs on the stator currents during a grid voltage dip. This dc-component delays the zero crossing of the current that flows through the circuit breaker. Fundamental property of the circuit breaker is that it can interrupt the current only when the current crosses the zero. The study is done utilizing the real-time simulation environment with protection relay-in-the-loop. Simulation results show that reactive current injection for voltage support purposes creates AC oscillations to the DFIG grid current. These oscillations advance the grid current zero crossing. This fact in turn improves the current interrupting capability of the wind turbine circuit breaker.

References

[1] T. Ackermann, Wind Power in Power Systems, John Wiley & Sons, Ltd, England, 2005.

[2] Vas, P. 1990. Vector Control of AC Machines. Clarendon Press Oxford. 327 p.

[3] Pena, R., Clare, J.C., Asher, G.M. Doubly Fed InductionGenerator using back-to-back PWM converters and its application to variable speed wind-energy generation.

[4] Jussila, M. 2007. Comparison of Space-Vector-Modulated Direct and Indirect Matrix Converters in Low-Power Applications. Thesis for the degree of Doctor of Technology. TUT, Tampere. 169 p.

[5] J.F. Conroy, R. Watson, Low-voltage ride through of a full converter wind turbine with permanent magnet generator, Renewable Power Generation, IET 1 (3) (2007) 182-189.

[6] A. Mäkinen, O. Raipala, K. Mäki, S. Repo, H. Tuusa, Fault ride through studies of full power converter wind turbine in a real time simulation environment, in: 5th Nordic Wind Power Conference 2009, NWPC'2009, Bornholm, Denmark, 2009, p. 8.

[7] E.ON Netz GmbH, Bayreuth, Grid Code, High and extra high voltage, Germany, 2006, p. 46.

[8] A. Mäkinen, H. Tuusa, Wind turbine and grid interaction studies using integrated real-time simulation environment, Proceedings of Nordic Workshop on Power and Industrial Electronics 2008, p. 8.

[9] A. S. Mäkinen, O. Raipala, K. Mäki, S. Repo, H. Tuusa, Fault ride-through capability of full-power converter wind turbine, Journal of Energy and Power Engineering, October 2010, Vol. 4, No. 10, David Publishing, USA, p. 17.

[10] A. S. Mäkinen, H. Tuusa, Effect of Transient Flux Compensation Control on Fault Ride Through of Doubly-Fed Induction Generator Wind Turbine, International Conference on Renewable Energies and Power Quality (ICREPQ'11), Las Palmas de Gran Canaria, Spain, p.6.

[11] A. S. Mäkinen, O. Raipala, S. Repo, H. Tuusa, Influence of DFIG reactive current injection during a voltage dip on the operation of wind turbine circuit breaker, 8th International Conference on Power Electronics – ECCE Asia, 2011, Jeju, Korea, p. 8.